PAPER

Transfer matrix method for optics in graphene layers

To cite this article: Tianrong Zhan *et al* 2013 *J. Phys.: Condens. Matter* **25** 215301

View the article online for updates and enhancements.

You may also like

- pn-Pair Avarage Velocity in Statistical Model of Photofission
  U. Lucia

- Relativistic and Thermodynamically Consistent Treatment for Finite-Volume Effect of Nucleons in Nuclear Matter (I) General Formulation
  Qi-Ren Zhang

- The Construction of q-Boson Realizations and q-Differential Realizations for Quantum Algebras
  Hong-Chen Fu

Recent citations

- Sensitivity Enhancement of Surface Plasmon Resonance Biosensor with 2-D Franckeite Nanosheets
  Bhishma Karki *et al*

- Skin effect photon-trapping enhancement in infrared photodiodes
  Haonan Ge *et al*

- 564: Design of a Transparent Dielectric Metamirror for Micro LED Displays
  Khaled Ahmed

Transfer matrix method for optics in graphene layers

Tianrong Zhan, Xi Shi, Yunyun Dai, Xiaohan Liu and Jian Zi

Department of Physics, Key Laboratory of Micro and Nano Photonic Structures (MOE), and State Key Laboratory of Surface Physics, Fudan University, Shanghai 200433, People's Republic of China

E-mail: jzi@fudan.edu.cn

Abstract
A transfer matrix method is developed for optical calculations of non-interacting graphene layers. Within the framework of this method, optical properties such as reflection, transmission and absorption for single-, double- and multi-layer graphene are studied. We also apply the method to structures consisting of periodically arranged graphene layers, revealing well-defined photonic band structures and even photonic bandgaps. Finally, we discuss graphene plasmons and introduce a simple way to tune the plasmon dispersion.

(Some figures may appear in colour only in the online journal)

1. Introduction

Graphene is a flat monolayer of graphite with carbon atoms closely packed in a two-dimensional honeycomb lattice. A hallmark of graphene is the existence of Dirac cones in the electronic band structure, resulting in extraordinary structural and electronic properties with great potential for nanoelectronics [1–3].

In addition to outstanding electrical, mechanical and chemical properties, graphene has interesting optical response. One of the striking optical properties of graphene is that its reflectance, transmittance and absorbance are determined by the fine structure constant [4, 5]. Despite being only one-atomic-layer thick with negligible reflection, a single free-standing graphene layer shows significant absorbance, universally about 2.2% in a spectral range from near-infrared to visible [4, 6, 7]. In the infrared regime, graphene absorption can be altered by applying gate voltages [8, 9]. For few-layer graphene, the optical absorption is proportional to the number of layers [10], leading to a visual image contrast which can be used practically to identify the number of graphene layers on a substrate. The highly transparent and outstanding electrical properties of graphene make it attractive for transparent electrodes [11, 12]. The broadband absorption implies that graphene has potential as an active medium for use in broadband photodetectors [13, 14], ultra-fast lasers [15] and optical modulation [16]. By applying

an external magnetic field, giant Faraday rotations can be generated in graphene [17, 18].

In doped or gated graphene, collective excitations—plasmons—exist with interesting optical features such as deep subwavelength and high confinement of optical fields [19–25], similar to surface plasmons in metal surfaces [26–28]. As a result, graphene may serve as a one-atom-thick platform for infrared and terahertz metamaterials [29, 30]. A number of photonic devices such as waveguides, splitters and combiners and superlenses could be envisioned [30, 31]. Numerical simulations suggest that periodically patterned arrays of doped graphene nanodisks may completely absorb infrared light at certain resonant wavelengths [32]; this was soon confirmed experimentally [33]. These interesting optical properties of graphene may also offer potential applications in photonics [34].

In this paper, we develop a transfer matrix method to study optical properties in non-interacting graphene layers. This paper is organized as follows. In section 2, we introduce the transfer matrix method to study the propagation of light through graphene layers, together with the optical conductivity of graphene used in our calculations. In sections 3–5, we apply the transfer matrix method to the study of optics in graphene layers. Specifically, in section 3 we discuss reflection, transmission and absorption in single-, double- and multi-layer graphene. In section 4, we discuss photonic band structures in periodical graphene layers. In
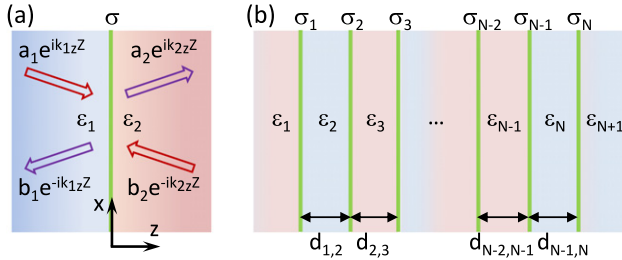
Figure 1. (a) A single graphene layer surrounded by two dielectrics with dielectric constants ε_1 and ε_2. The graphene layer is characterized by a conductivity σ. Red and purple arrows indicate incoming and outgoing light, respectively. (b) A stack of N graphene layers of conductivity σ_i ($i = 1, 2, \ldots, N$) which are separated by different dielectrics with dielectric constants ε_i ($i = 1, 2, \ldots, N + 1$). The spacing between two adjacent graphene layers is denoted by $d_{i,i+1}$ ($i = 1, 2, \ldots, N - 1$).

section 5, we discuss plasmons in graphene. Finally, we present our summary in section 6.

2. General formulation

The transfer matrix method is a powerful tool in the analysis of light propagation through layered dielectric media [35, 36]. The central idea lies in the fact that electric or magnetic fields in one position can be related to those in other positions through a transfer matrix. Within the framework of the transfer matrix method, there are two kinds of matrices: one is the transmission matrix that connects the fields across an interface and the other is the propagation matrix that connects the fields propagating over a distance within a homogeneous medium.

2.1. Transmission matrix

We first consider the propagation of light across an interface formed by a graphene layer that separates two dielectrics with dielectric constants ε_1 and ε_2, as shown schematically in figure 1(a). The graphene layer has an optical conductivity σ lying at $z = 0$. Light is assumed to be polarized in the y direction and to propagate in the z direction. For the structures considered, the s and p polarizations can be decoupled. As a result, we can deal with the s and p polarizations separately.

For p polarization, the magnetic field is polarized along the y direction and can be written as the form

$$H_{1y} = (a_1 e^{ik_{1z}z} + b_1 e^{-ik_{1z}z}) e^{ik_{1x}x}, \qquad z < 0, \quad (1)$$

$$H_{2y} = (a_2 e^{ik_{2z}z} + b_2 e^{-ik_{2z}z}) e^{ik_{2x}x}, \qquad z > 0. \quad (2)$$

Here, a_i and b_i ($i = 1, 2$) are the field coefficients, k_{ix} (k_{iz}) is the x (z) component of the wavevector $k_i = \sqrt{\varepsilon_i}\omega/c$, where ω is the angular frequency and c is the speed of light in vacuum. The first (second) term in the parentheses on the right-hand side represents waves propagating along the z ($-z$) direction. From Snell's law, we will immediately have $k_{1x} = k_{2x}$.

The electric and magnetic fields at the interface can be related by the following boundary conditions [37]:

$$\mathbf{n} \times (\mathbf{E}_2 - \mathbf{E}_1)|_{z=0} = 0, \quad (3)$$

$$\mathbf{n} \times (\mathbf{H}_2 - \mathbf{H}_1)|_{z=0} = \mathbf{J}, \quad (4)$$

where $\mathbf{n}$ is the unit surface normal and $\mathbf{J}$ is the surface current density of the graphene layer. Applying the above boundary conditions at $z = 0$, we will have

$$\frac{k_{1z}}{\varepsilon_1}(a_1 - b_1) - \frac{k_{2z}}{\varepsilon_2}(a_2 - b_2) = 0, \quad (5)$$

$$(a_1 + b_1) - (a_2 + b_2) = J_x. \quad (6)$$

Note that $\mathbf{J}$ can be obtained from Ohm's law, namely

$$J_x = \sigma E_x|_{z=0} = \frac{\sigma k_{2z}}{\varepsilon_0 \varepsilon_2 \omega}(a_2 - b_2), \quad (7)$$

where ε_0 is the vacuum permittivity. Combining equations (5)–(7), the coefficients a_1 and b_1 can be related to a_2 and b_2 by a 2×2 transmission matrix $D_{1 \to 2}$,

$$\begin{bmatrix} a_1 \\ b_1 \end{bmatrix} = D_{1 \to 2} \begin{bmatrix} a_2 \\ b_2 \end{bmatrix}, \quad (8)$$

where

$$D_{1 \to 2} = \frac{1}{2} \begin{bmatrix} 1 + \eta_p + \xi_p & 1 - \eta_p - \xi_p \\ 1 - \eta_p + \xi_p & 1 + \eta_p - \xi_p \end{bmatrix}, \quad (9)$$

with the parameters η_p and ξ_p given by

$$\eta_p = \frac{\varepsilon_1 k_{2z}}{\varepsilon_2 k_{1z}}, \qquad \xi_p = \frac{\sigma k_{2z}}{\varepsilon_0 \varepsilon_2 \omega}. \quad (10)$$

For s polarization, the electric field is polarized along the y direction. Similarly, by applying the boundary conditions and Ohm's law, the transmission matrix for s polarization that relates the electric fields at the two sides of the interface can be obtained, as

$$D_{1 \to 2} = \frac{1}{2} \begin{bmatrix} 1 + \eta_s + \xi_s & 1 - \eta_s + \xi_s \\ 1 - \eta_s - \xi_s & 1 + \eta_s - \xi_s \end{bmatrix}, \quad (11)$$

with the parameters η_s and ξ_s given by

$$\eta_s = \frac{k_{2z}}{k_{1z}}, \qquad \xi_s = \frac{\sigma \mu_0 \omega}{k_{1z}}, \quad (12)$$

where μ_0 is the vacuum permeability.

The transmission matrices for s and p polarizations across an interface have similar forms except for the sign of ξ in the off-diagonal elements. Introducing a polarization dependent parameter ς_m, the transmission matrices for both polarizations can have an identical form,

$$D_{1 \to 2, m} = \frac{1}{2} \begin{bmatrix} 1 + \eta_m + \xi_m & 1 - \eta_m - \varsigma_m \xi_m \\ 1 - \eta_m + \varsigma_m \xi_m & 1 + \eta_m - \xi_m \end{bmatrix}, \quad (13)$$

where $m = (s, p)$ and $\varsigma_p = 1$ and $\varsigma_s = -1$.

2.2. Propagation matrix

We now consider the propagation of light in a homogeneous medium. It can be shown [35] that the electric or magnetic

fields at $z + \Delta z$ can be related to those at the z position by a 2×2 propagation matrix

$$P(\Delta z) = \begin{bmatrix} e^{-ik_z \Delta z} & 0 \\ 0 & e^{ik_z \Delta z} \end{bmatrix}. \tag{14}$$

2.3. Transfer matrix for multi-layer graphene

For the stack of N graphene layers shown in figure 1(b), the transfer matrix can be obtained by transmission matrices across different interfaces and propagation matrices in different homogeneous dielectric media. Denote the field coefficients on the left side of the leftmost graphene layer by a_1 and b_1 and those on the right side of the rightmost graphene layer by a_{N+1} and b_{N+1}. The two sets of field coefficients are then related by a 2×2 transfer matrix $\mathcal{M}$, namely

$$\begin{bmatrix} a_1 \\ b_1 \end{bmatrix} = \mathcal{M} \begin{bmatrix} a_{N+1} \\ b_{N+1} \end{bmatrix}, \tag{15}$$

with

$$\mathcal{M} = D_{1 \to 2} P(d_{1,2}) D_{2 \to 3} P(d_{2,3}) \cdots P(d_{N-1,N}) D_{N \to N+1}. \tag{16}$$

2.4. Scattering matrix

In certain cases, a better approach is to work with a scattering matrix [38] rather than a transfer matrix. The transfer matrix relates both the incoming and the outgoing waves on one side of a structure to those on the other side of the structure. In contrast, the scattering matrix $\mathcal{S}$ relates the outgoing waves to the incoming waves, for the multi-layer graphene shown in figure 1(b), given by

$$\begin{bmatrix} b_1 \\ a_{N+1} \end{bmatrix} = \mathcal{S} \begin{bmatrix} a_1 \\ b_{N+1} \end{bmatrix}. \tag{17}$$

From the transfer matrix, it is easy to obtain the scattering matrix

$$\mathcal{S} = \begin{bmatrix} M_{21}/M_{11} & (M_{11}M_{22} - M_{12}M_{21})/M_{11} \\ 1/M_{11} & -M_{12}/M_{11} \end{bmatrix}, \tag{18}$$

where $M_{i,j}$ $(i, j = 1, 2)$ are the elements of $\mathcal{M}$.

2.5. Optical spectrum calculations

With the transfer matrix, we can easily calculate the optical spectra such as reflection, transmission and absorption for multi-layer graphene. Suppose that light is incident from the left upon the multi-layer graphene with the reflection and transmission coefficients denoted respectively by r and t. It can be shown that these coefficients are given by the elements of $\mathcal{M}$,

$$r = \frac{M_{21}}{M_{11}}, \tag{19}$$

$$t = \frac{1}{M_{11}}. \tag{20}$$

The reflectance and transmittance can be calculated for both s and p polarizations as

$$R_{s,p} = |r_{s,p}|^2, \tag{21}$$

$$T_{s,p} = \eta_{s,p}|t_{s,p}|^2, \tag{22}$$

where

$$\eta_s = k_{(N+1)z}/k_{1z}, \qquad \eta_p = \varepsilon_1 k_{(N+1)z}/\varepsilon_{N+1} k_{1z}. \tag{23}$$

The absorbance can then be readily obtained from

$$A = 1 - R - T. \tag{24}$$

2.6. Optical conductivity of graphene

For illustration and simplicity, in this work we only consider the situation where the absolute value of the chemical potential of graphene μ is much larger than kT, where k is the Boltzmann constant and T is the temperature. In this situation, within the random-phase approximation the optical conductivity of graphene $\sigma(\omega)$ is given by [19–21, 39–41]

$$\frac{\sigma(\Omega)}{\varepsilon_0 c} = 4\alpha \frac{i}{\Omega} + \pi\alpha \left[\vartheta(\Omega - 2) + \frac{i}{\pi} \ln \left| \frac{\Omega - 2}{\Omega + 2} \right| \right]. \tag{25}$$

Here, $\Omega \equiv \hbar\omega/\mu$ is the dimensionless frequency, $\alpha \equiv e^2/4\pi\varepsilon_0\hbar c$ $(\sim 1/137)$ is the fine structure constant and $\vartheta(x)$ is the Heaviside step function. The first and second terms on the right-hand side stem from the intraband and interband contributions, respectively.

3. Reflection, transmission and absorption

3.1. Single-layer graphene

For a single graphene layer surrounded by two dielectrics with dielectric constants ε_1 and ε_2, suppose that light is incident from the dielectric medium of ε_1. The transfer matrix is nothing other than the transmission matrix across the interface, given by equations (9) and (11) for p and s polarizations, respectively. From equations (21) and (22), the reflectance and transmittance can be obtained as

$$R_s = \left| \frac{\sqrt{\varepsilon_1} \cos\theta_1 - \sqrt{\varepsilon_2} \cos\theta_2 - \widetilde{\sigma}}{\sqrt{\varepsilon_1} \cos\theta_1 + \sqrt{\varepsilon_2} \cos\theta_2 + \widetilde{\sigma}} \right|^2, \tag{26}$$

$$R_p = \left| \frac{\sqrt{\varepsilon_2}/\cos\theta_2 - \sqrt{\varepsilon_1}/\cos\theta_1 + \widetilde{\sigma}}{\sqrt{\varepsilon_2}/\cos\theta_2 + \sqrt{\varepsilon_1}/\cos\theta_1 + \widetilde{\sigma}} \right|^2, \tag{27}$$

$$T_s = \frac{4\sqrt{\varepsilon_1\varepsilon_2} \cos\theta_1 \cos\theta_2}{\left| \sqrt{\varepsilon_1} \cos\theta_1 + \sqrt{\varepsilon_2} \cos\theta_2 + \widetilde{\sigma} \right|^2}, \tag{28}$$

$$T_p = \frac{4\sqrt{\varepsilon_1\varepsilon_2}/(\cos\theta_1 \cos\theta_2)}{\left| \sqrt{\varepsilon_2}/\cos\theta_2 + \sqrt{\varepsilon_1}/\cos\theta_1 + \widetilde{\sigma} \right|^2}, \tag{29}$$

where θ_1 and θ_2 are the incident and refracted angles, respectively, and $\widetilde{\sigma} = \sigma/\varepsilon_0 c$. By neglecting the higher-order terms of $\widetilde{\sigma}$, the absorbance is given by

$$A_s = \frac{4\sqrt{\varepsilon_1} \cos\theta_1 \text{Re}(\widetilde{\sigma})}{\left(\sqrt{\varepsilon_1} \cos\theta_1 + \sqrt{\varepsilon_2} \cos\theta_2 + \widetilde{\sigma} \right)^2}, \tag{30}$$
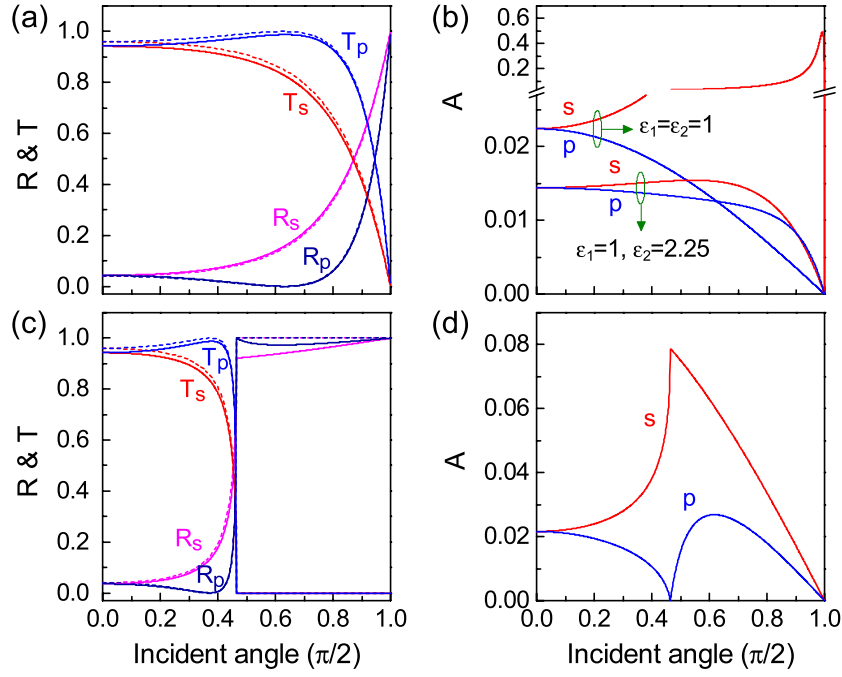
Figure 2. The reflectance, transmittance and absorbance of single-layer graphene as a function of the incident angle for $\Omega > 2$. (a) Reflectance and transmittance for s and p polarizations with $\varepsilon_1 = 1$ and $\varepsilon_2 = 2.25$. The dashed lines represent the situation in the absence of the graphene layer. (b) Absorbance for (i) $\varepsilon_1 = \varepsilon_2 = 1$ and (ii) $\varepsilon_1 = 1$ and $\varepsilon_2 = 2.25$. (c) The same as (a) but for $\varepsilon_1 = 2.25$ and $\varepsilon_2 = 1$. The corresponding absorbance is given in (d).

$$A_p = \frac{4\sqrt{\varepsilon_1}\mathrm{Re}(\tilde{\sigma})/\cos\theta_1}{\left(\sqrt{\varepsilon_2}/\cos\theta_2 + \sqrt{\varepsilon_1}/\cos\theta_1 + \tilde{\sigma}\right)^2}. \qquad (31)$$

Obviously, for a single free-standing graphene layer under normal incidence the absorbance for $\Omega > 2$ is given by $\pi\alpha/(1 + \pi\alpha/2)^2 \sim \pi\alpha$.

In figure 2, the reflectance, transmittance and absorbance at different incident angles for single graphene are shown. Light is incident from the dielectric of ε_1. The reflection and transmission are altered somewhat with respect to the case without the graphene layer. For $\varepsilon_1 \leq \varepsilon_2$, the absorbance decreases monotonically with increasing incident angle for p polarization, while for s polarization it increases up to a maximum and then decreases monotonically. For $\varepsilon_1 = \varepsilon_2$, the absorbance for s polarization takes a universal value at normal incidence, about $\pi\alpha$, and the maximal absorbance is 0.5 at an incident angle very close to $\pi/2$.

For $\varepsilon_1 > \varepsilon_2$, total internal reflection is expected. With the presence of the graphene layer, there is nearly no change in the critical angle. However, above the critical angle the reflectance is no longer *total* (smaller than one). For s polarization, the absorbance around the critical angle is several times larger than the universal value of $\pi\alpha$. This implies that the configuration of total internal reflection could be exploited in measurements of optical conductivity of graphene since it can suppress the signal-to-noise ratio considerably.

3.2. Double-layer graphene

Consider two graphene layers which are separated by a dielectric of ε_2 with a thickness of d. The dielectric constant of

the leftmost dielectric is ε_1 and that of the rightmost dielectric is ε_3. The transfer matrix of the structure can be obtained from equation (16) as

$$\mathcal{M} = D_{1\to2}P(d)D_{2\to3}, \qquad (32)$$

the elements of which are given by

$$M_{\mu\nu,m} = \frac{\cos k_{2z}d}{2}A_{\mu\nu,m} + \frac{\mathrm{i}\sin k_{2z}d}{2}B_{\mu\nu,m}, \qquad (33)$$

where $\mu = 1, 2$ and $\nu = 1, 2$. The parameters $A_{\mu\nu,m}$ and $B_{\mu\nu,m}$ are given by

$$A_{\mu\nu,m} = 1 + (-1)^{\mu+\nu}\eta_m\eta'_m - (-1)^\nu\left(\xi'_m + \varsigma_m\xi_m\eta'_m\right), \quad (34)$$

$$B_{\mu\nu,m} = (-1)^\mu\eta_m + (-1)^\nu\left(\eta'_m + \varsigma_m\xi_m\eta'_m\right)$$
$$- (-1)^{\mu+\nu}\eta_m\xi'_m - \varsigma_m\xi_m, \qquad (35)$$

where

$$
\begin{array}{ll}
\eta_s = k_{2z}/k_{1z}, & \eta_p = \varepsilon_1 k_{2z}/\varepsilon_2 k_{1z}, \\
\xi_s = \sigma\mu_0\omega/k_{1z}, & \xi_p = \sigma k_{2z}/\varepsilon_0\varepsilon_2\omega, \\
\eta'_s = k_{3z}/k_{2z}, & \eta'_p = \varepsilon_2 k_{3z}/\varepsilon_3 k_{2z}, \\
\xi'_s = \sigma\mu_0\omega/k_{2z}, & \xi'_p = \sigma k_{3z}/\varepsilon_0\varepsilon_3\omega.
\end{array}
\qquad (36)
$$

In figure 3, the reflectance, transmittance and absorbance of double-layer graphene for $\varepsilon_1 = \varepsilon_3 = 1$ and $\varepsilon_2 = 2.25$ are shown. For small d, despite different values, the dependences of the reflectance, transmittance and absorbance on the incident angle are, in general, similar to those of single-layer graphene. At normal incidence, the absorbance is nearly twice the universal value of $\pi\alpha$. For large d, however, there are oscillations in the reflectance, transmittance and absorbance, which originate from the thin-film interference.
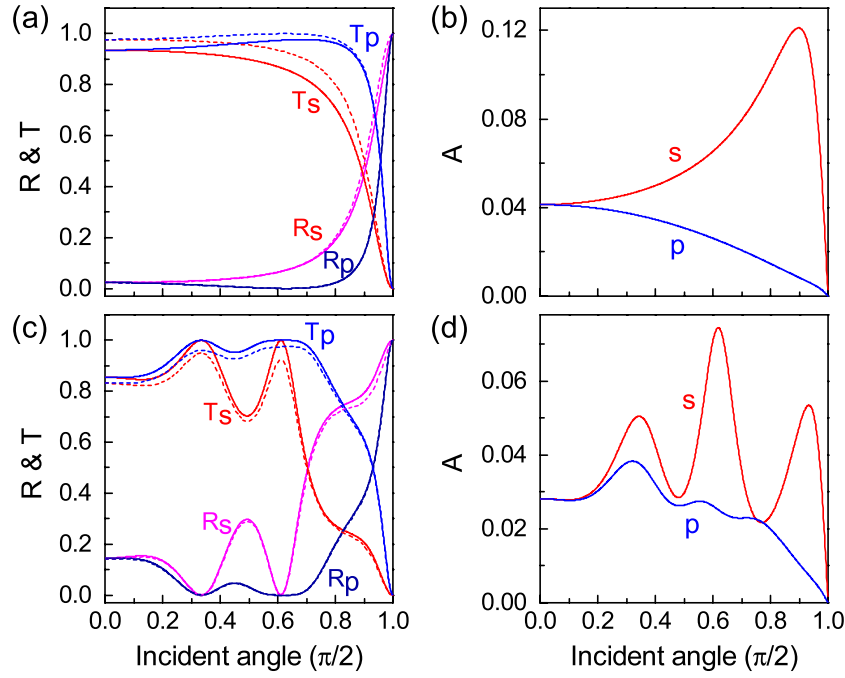
Figure 3. The reflectance, transmittance and absorbance of double-layer graphene as a function of the incident angle for $\Omega > 2$. The two graphene layers have the same optical conductivity. (a) Reflectance and transmittance for s and p polarizations with $d = 0.1\hbar c/\mu$ (corresponding to 0.132 μm for a typical chemical potential $\mu = 0.15$ eV). The dashed lines represent the situation in the absence of the graphene layers. The corresponding absorbance is given in (b). (c) The same as (a) but for $d = 8\hbar c/\mu$ (corresponding to 10.5 μm for $\mu = 0.15$ eV). The corresponding absorbance is given in (d).

3.3. Multi-layer graphene

For multi-layer graphene, the transfer matrix can be obtained from equation (16). The reflectance, transmittance and absorbance can then be obtained from equations (21), (22) and (24) respectively.

In figure 4, the reflectance and absorbance of multi-layer graphene at normal incidence are shown. The structure consists of identical graphene layers in air, separated equally by a distance d. At low frequencies the reflectance is close to one up to a certain cutoff frequency. Above the cutoff frequency, for small d the reflectance oscillates and drops rapidly to zero. For large d, however, there appear sharp reflection peaks for frequencies above the cutoff frequency, resulting from the multiple interference by the graphene layers.

The structure has zero absorbance for $\Omega < 2$ and shows remarkable absorption for $\Omega > 2$. For small d, the absorbance is nearly a constant for $\Omega > 2$. With increasing d, multiple interference by the graphene layers may play an important role, leading to sharp absorption dips. These interesting properties imply that multi-layer graphene has potential as a dark material to achieve lower reflection coatings and enhanced photodetection [42].

3.4. Comparison with two-dimensional electron gas

In graphene, the electron band structure is characterized by Dirac cones showing linear dispersion, different from that in conventional two-dimensional electron gas (2DEG) with
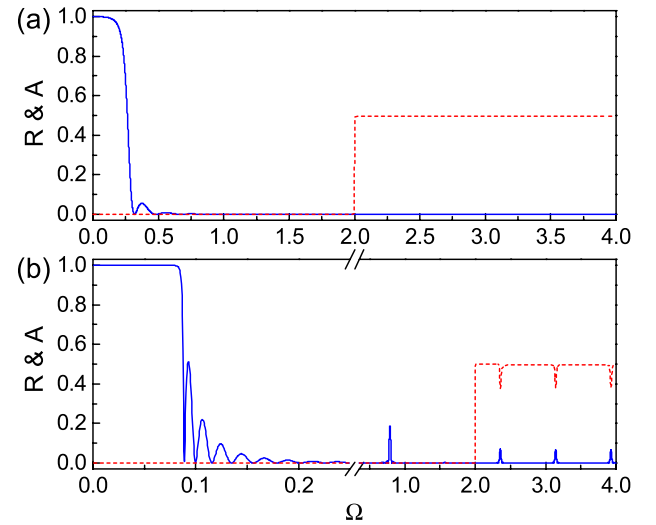

Figure 4. The reflectance (solid line) and absorbance (dashed line) spectra of 30 graphene layers at normal incidence. (a) $d = 0.4\hbar c/\mu$ and (b) $d = 4\hbar c/\mu$ (corresponding to 0.132 and 5.26 μm for $\mu = 0.15$ eV, respectively).

parabolic dispersion. This difference will lead to different polarizability and hence optical conductivity [43, 44]. In 2DEG, the optical conductivity has exactly the same form as the intraband contribution in graphene (the first term on the right-hand side of equation (25)), differing in the interband contribution from graphene (the second term on the right-hand side of equation (25)). As a result, the optical properties of graphene may differ from those of 2DEG.
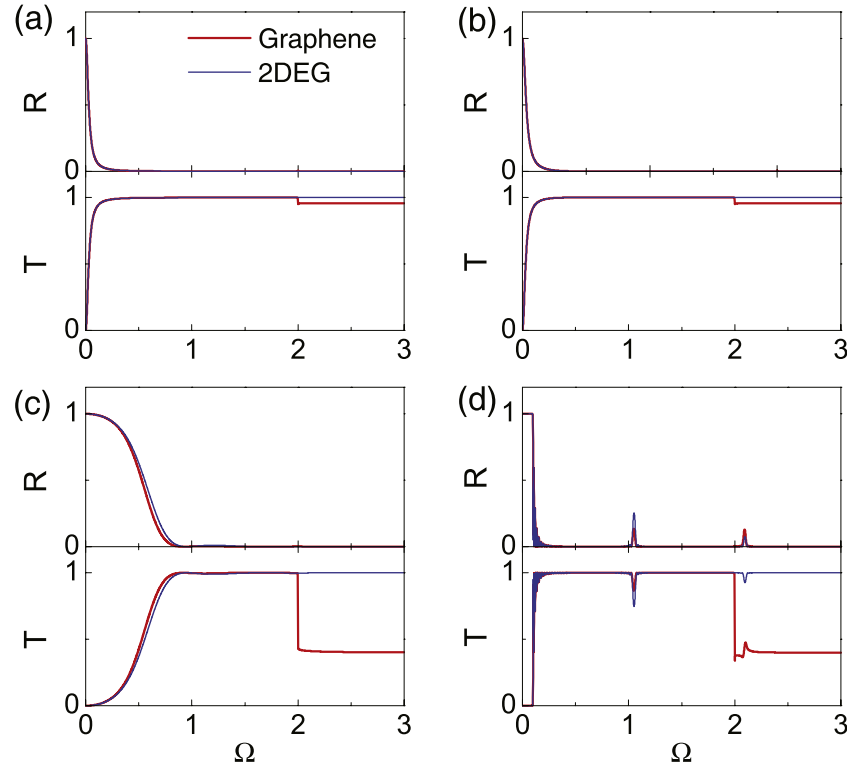
Figure 5. Comparison of reflection and transmission spectra between graphene and 2DEG layers at normal incidence. (a), (b) Two graphene and 2DEG layers with $d = 0.1\hbar c/\mu$ and $d = 3\hbar c/\mu$, respectively. (c), (d) 40 graphene and 2DEG layers with $d = 0.1\hbar c/\mu$ and $d = 3\hbar c/\mu$, respectively.

In figure 5, a comparison of reflection and transmission properties between graphene and 2DEG layers is shown. For both systems, the layers of identical optical conductivity are separated equally by a distance d. The results for 2DEG are also calculated within the same framework of the developed transfer matrix method but with a different optical conductivity. The reflection and transmission spectra between graphene and 2DEG layers for both small and large d are very similar in the frequency range $\Omega < 2$. There is a difference for $\Omega > 2$. This is not surprising since for $\Omega > 2$ interband excitations are expected in graphene, which are absent in 2DEG. In many studies [30, 31], graphene is modelled by an ultrathin metal with the optical conductivity of 2DEG. Our results indicate that this analogy is reasonable and valid for $\Omega < 2$.

4. The photonic band structure of periodical graphene layers

When dielectrics are arranged in a periodical way to form so-called photonic crystals [45–47], electromagnetic waves should be strongly modulated by Bragg scatterings, showing photonic band structures with well-defined photonic bands and even photonic bandgaps. For graphene layers stacked in a periodical way, photonic band structures should also be expected due to the introduced periodical modulations.

The first structure considered is shown schematically in figure 6(a). It is composed of identical graphene layers embedded into the interfaces of a one-dimensional photonic crystal consisting of two dielectrics with dielectric constants of ε_1 and ε_2 and thicknesses of d_1 and d_2, respectively. For such a structure, the transfer matrix after propagating over one unit cell reads

$$\mathcal{M}_m = D_{1 \to 2,m} P(d_2) D_{2 \to 1,m} P(d_1). \tag{37}$$

The photonic band structure can then be obtained from the diagonal elements of the transfer matrix [36], $\cos(qd) = \left(M_{11,m} + M_{22,m}\right)/2$, where q is the Bloch wavevector and $d = d_1 + d_2$ is the lattice constant. It can be explicitly written as

$$\cos(qd) = \cos(k_{1z}d_1)\cos(k_{2z}d_2) - \tfrac{1}{2}(\eta_m + \eta_m^{-1})$$
$$\times \sin(k_{1z}d_1)\sin(k_{2z}d_2) - \Delta_m, \tag{38}$$

where

$$\Delta_m = \mathrm{i}\xi_m[(1 + \eta_m^{-1})\sin(k_{1z}d_1 + k_{2z}d_2)$$
$$+ \varsigma_m(1 - \eta_m^{-1})\sin(k_{1z}d_1 - k_{2z}d_2)]$$
$$+ \frac{\xi_m^2}{2\eta_m}\sin(k_{1z}d_1)\sin(k_{2z}d_2). \tag{39}$$

Without the term Δ_m, equation (38) reduces to the photonic band structure of a one-dimensional photonic crystal [36].

For identical graphene layers separated equally by a distance d in air, as shown in figure 6(b), the transfer matrix simply reads $\mathcal{M}_m = D_m P(d)$, where

$$D_m = \begin{bmatrix} 1 + \xi_m/2 & -\varsigma_m\xi_m/2 \\ \varsigma_m\xi_m/2 & 1 - \xi_m/2 \end{bmatrix}. \tag{40}$$
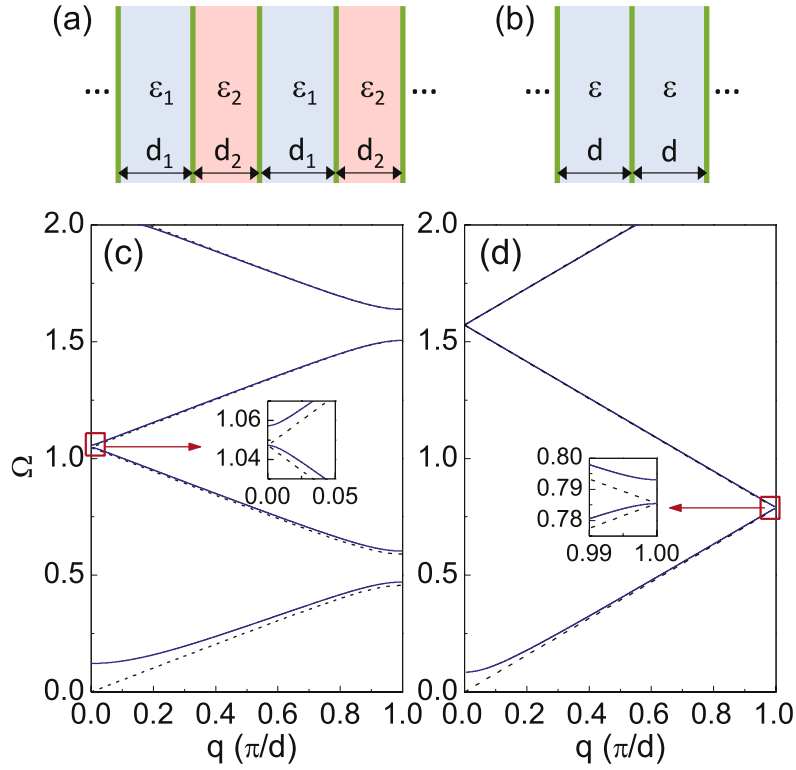
Figure 6. (a) Schematic of a structure consisting of identical graphene layers placed at the interfaces of a one-dimensional photonic crystal. (b) Schematic of a structure consisting of identical graphene layers separated equally in air. (c) Photonic band structure (solid lines) for the structure in (a). The parameters are $\varepsilon_1 = 1$, $\varepsilon_2 = 2.25$, $d_1 = 3\hbar c/\mu$ and $d_2 = 2\hbar c/\mu$ (corresponding to 2.63 and 3.95 μm for $\mu = 0.1$ eV, respectively). The dashed lines are the results in the absence of graphene layers. (d) The same as (c) but for the structure in (b). The parameters are $\varepsilon = 1$ and $d = 4\hbar c/\mu$. The dashed lines are simply the folded dispersion in air, $\omega = qc$.

The photonic band structure of the structure is then given by

$$\cos(qd) = \cos(k_z d) - \frac{\mathrm{i}\xi_m}{2}\sin(k_z d), \qquad (41)$$

which is identical to that given in [48].

In figure 6, the photonic band structures of periodical graphene layers are shown for the propagation direction perpendicular to the graphene layers. For both structures the first photonic band starts from a certain nonzero cutoff frequency, different from conventional dielectric photonic crystals. This cutoff frequency corresponds exactly to that observed in the reflection spectra shown in figure 4. Below the cutoff frequency, high reflection or low transmission is expected, which was also observed in numerical simulations of a stack of graphene layers separated by dielectric slabs [49]. It is known that in the low-frequency limit periodical metallic structures can be considered as bulk metals with depressed effective plasma frequencies [50, 51]. Thus, periodical graphene layers can also be regarded as a bulk metal with an extremely low effective plasma frequency.

For the structure shown in figure 6(a), the photonic crystal in the absence of graphene layers displays well-defined photonic bands and bandgaps. With the introduction of graphene layers, however, both the photonic bands and the bandgaps are modified. For example, for the photonic crystal in the absence of graphene layers, there should be no bandgap between the second and third photonic bands since this

photonic crystal is a quarter-wave stack. In the presence of graphene layers, however, a mini photonic bandgap opens up.

For the second structure shown in figure 6(b), there should be no photonic bandgaps in the absence of graphene layers. In the presence of graphene layers, however, a series of mini photonic bandgaps appears owing to the multiple interference by the graphene layers. It is known that for frequencies within photonic bandgaps light propagation is forbidden [45–47]. For a structure consisting of finite graphene layers, this will cause strong reflection for frequencies located in the mini photonic bandgaps, as can be clearly seen from figure 4(b).

5. Plasmons

A flat metal surface can support surface plasmons [26–28], which are transverse magnetic (TM) electromagnetic waves coupled with collective oscillations of surface charges. Surface plasmons can propagate along the metal surface with the fields decaying exponentially away from both sides of the surface. In doped or gated graphene, free carriers can also support plasmons [19–24]. Owing to its two-dimensional nature and unique electronic band structure, graphene can support not only TM but also transverse electric (TE) plasmons [21]. The latter do not exist in conventional metal surfaces.

For a graphene layer surrounded by two dielectrics, as shown in figure 1(a), the transfer matrix is simply the transmission matrix. From equation (19), the reflection coefficient of the system can be obtained. The condition for the existence of plasmons is that the reflection coefficient has poles, namely

$$1 + \eta_m + \varsigma_m \xi_m = 0, \tag{42}$$

where the subscript m stands for s and p polarization, corresponding to the TE and TM modes, respectively.

From equation (42), the dispersion of TM plasmons can be obtained as

$$\frac{\varepsilon_1}{\sqrt{Q^2 - \varepsilon_1 \Omega^2}} + \frac{\varepsilon_2}{\sqrt{Q^2 - \varepsilon_2 \Omega^2}} = -\frac{\mathrm{i}\sigma(\Omega)/\varepsilon_0 c}{\Omega}, \tag{43}$$

with $Q \equiv \hbar c q/\mu$, where $q(\equiv k_x)$ is the wavevector of the plasmons. Obviously, TM plasmons can exist if the imaginary part of σ is *positive*. From the above equation, TM plasmons are far below the light line, i.e., $q \gg \omega/c$. Thus, in this non-retarded regime, the dispersion of TM plasmons is simplified to

$$Q = -(\varepsilon_1 + \varepsilon_2)\,\Omega\,(\varepsilon_0 c)/\mathrm{i}\sigma. \tag{44}$$

For $\Omega > 2$, σ has a real value as well, leading to a strong loss due to interband excitations. For small q, the dispersion of TM plasmons reduces to

$$\Omega = 2\sqrt{\frac{\alpha}{(\varepsilon_1 + \varepsilon_2)}Q}, \tag{45}$$

which shows the known $\sqrt{q}$-dependence [19, 20].

From equation (42), the dispersion of TE plasmons is given by

$$\sqrt{Q^2 - \varepsilon_1 \Omega^2} + \sqrt{Q^2 - \varepsilon_2 \Omega^2} = \frac{\mathrm{i}\sigma}{\varepsilon_0 c}\Omega, \tag{46}$$

which is the same as that given in [21]. TE plasmons can exist if $\varepsilon_1 = \varepsilon_2$ and the imaginary part of σ is *negative* (for $\Omega > 1.667$). Note that the term on the right-hand side of the above equation is very small in the frequency window $1.667 < \Omega < 2$. As a result, the dispersion of TE plasmons should be below but very close to the light line $\omega = qc/\sqrt{\varepsilon_1}$.

We now consider a structure where a graphene layer is separated from a dielectric substrate with ε_2 by a distance d, as shown schematically in the inset of figure 7. For this structure, TE plasmons do not exist for finite d and thus we only discuss TM plasmons. For p polarization, the transfer matrix of the structure can be obtained from equation (16), namely

$$\mathcal{M} = DP(d)D', \tag{47}$$

where

$$D = \frac{1}{2}\begin{bmatrix} 1 + \eta_p + \xi_p & 1 - \eta_p - \xi_p \\ 1 - \eta_p + \xi_p & 1 + \eta_p - \xi_p \end{bmatrix}, \tag{48}$$

$$D' = \frac{1}{2}\begin{bmatrix} 1 + \eta_p' & 1 - \eta_p' \\ 1 - \eta_p' & 1 + \eta_p' \end{bmatrix}, \tag{49}$$

$$P = \begin{bmatrix} \mathrm{e}^{-\mathrm{i}k_{1z}d} & 0 \\ 0 & \mathrm{e}^{\mathrm{i}k_{1z}d} \end{bmatrix}, \tag{50}$$
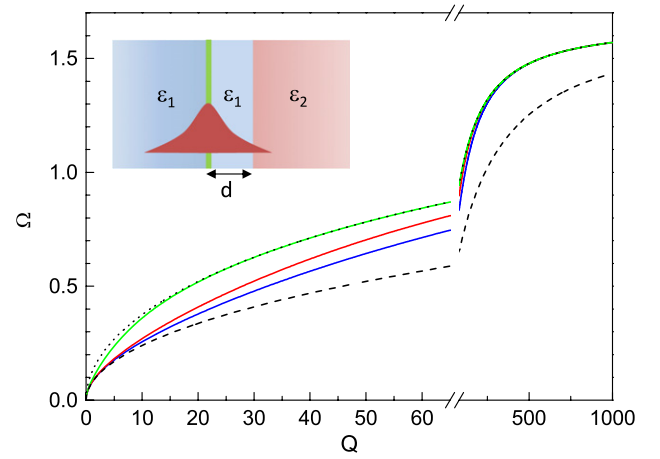

Figure 7. The dispersion of TM plasmons for the structure shown in the inset, where the graphene layer is separated from a dielectric substrate with $\varepsilon_2 = 10$ by a distance d and the other dielectrics are air with $\varepsilon_1 = 1$. The blue, green and red lines are the results for $\tilde{d} = 0.005, 0.01$ and 0.1, respectively. The dotted line represents the dispersion for a free-standing graphene layer in air and the dashed line corresponds to the case $d = 0$.

with

$$\eta_p = 1, \qquad \xi_p = \sigma k_{1z}/\varepsilon_0 \varepsilon_1 \omega,$$
$$\eta_p' = \varepsilon_1 k_{2z}/\varepsilon_2 k_{1z}. \tag{51}$$

With the transfer matrix, it is easy to obtain the reflection coefficient from equation (19). The condition for the existence of plasmons thus reads

$$\left(1 + \eta_p + \xi_p\right)\left(1 + \eta_p'\right)\mathrm{e}^{-\mathrm{i}k_{1z}d}$$
$$+ \left(1 - \eta_p - \xi_p\right)\left(1 - \eta_p'\right)\mathrm{e}^{\mathrm{i}k_{1z}d} = 0. \tag{52}$$

Since the dispersion of graphene plasmons lies far below the light line, the non-retarded condition $q \gg \omega/c$ still holds, leading to $\eta_p' \simeq \varepsilon_1/\varepsilon_2$ and $\xi_p \simeq \mathrm{i}\sigma q/\varepsilon_0 \varepsilon_1 \omega$. Thus, the plasmon dispersion can be simplified as

$$\frac{2\varepsilon_1(\varepsilon_1 + \varepsilon_2)}{(\varepsilon_1 + \varepsilon_2) + (\varepsilon_1 - \varepsilon_2)\,\mathrm{e}^{-2Q\tilde{d}}} = -\frac{\mathrm{i}\sigma}{\varepsilon_0 c}\frac{Q}{\Omega}, \tag{53}$$

where $\tilde{d} = d\mu/\hbar c$.

In figure 7, the dispersion of TM plasmons for the structure shown in the inset is given. The separation of the graphene layer from the dielectric substrate with ε_2 considerably affects the dispersion. For small q, the dispersion is that for the case of $d = 0$. For large q, it approaches that for the free-standing case. This dispersion interchange with increasing q can be understood from the fact that the fields of plasmons decay exponentially into the surrounding media, as schematically depicted in the inset. For small q, the decay length is much larger than d, such that the fields concentrate dominantly in the substrate. As a result, the dispersion should be that for the case $d \sim 0$. For large q, the fields decay very rapidly, such that the decay length is much smaller than d. In this situation, the fields cannot sense the substrate dielectric layer.

Obviously, the dispersion interchange can be tuned by d. The change from one kind of dispersion to the other occurs faster for large d than for small d. Practically, we may adopt this dispersion interchange to tune the dispersion of TM plasmons or, in other words, the refractive index of the plasmons. From equation (44), the corresponding refractive index of TM plasmons for a graphene layer surrounded by two dielectrics with ε_1 and ε_2 is given by

$$n_{\mathrm{p}} \equiv qc/\omega = -\frac{\varepsilon_1 + \varepsilon_2}{\mathrm{i}\sigma/\varepsilon_0 c}. \tag{54}$$

With the structure shown in the inset of figure 7, the refractive index of TM plasmons can thus be tuned from $-2\varepsilon_1/\left(\mathrm{i}\sigma/\varepsilon_0 c\right)$ to $-\left(\varepsilon_1 + \varepsilon_2\right)/\left(\mathrm{i}\sigma/\varepsilon_0 c\right)$. This offers a simple approach to manipulate the dispersion of TM plasmons or the refractive index practically by changing d [52].

6. Conclusions

In this paper, we developed a transfer matrix method for optical calculations in non-interacting graphene layers. Within the framework of this method, the transfer matrices for various graphene layers can be obtained, from which the reflectance, transmittance and absorbance spectra of graphene layers can be easily obtained. In addition, photonic band structures for periodical graphene layers and even graphene plasmons can be studied in a rather simple way.

Using the transfer matrix method, we studied the optical properties such as reflection, transmission and absorption for single-, double- and multi-layer graphene. We showed that the configuration of total internal reflection in single-layer graphene and thin-film interference effects in double-layer graphene could be exploited to enhance the light absorption. For multi-layer graphene, there exists a cutoff frequency below which the reflectance is as high as one. For a small spacing distance, the absorption is very large for $\Omega > 2$. With increasing spacing distance, sharp reflection peaks and absorption dips appear owing to the multiple interference by the graphene layers.

We applied the transfer matrix method to structures consisting of periodically arranged identical graphene layers. The structures are characterized by photonic band structures with well-defined photonic bands and bandgaps. We revealed that these structures can be regarded as bulk metals with extremely low effective plasma frequencies.

Finally, we discussed plasmons in a graphene layer that is separated from a dielectric substrate. We found that the plasmon dispersion can be tuned by the separation between the graphene layer and the dielectric substrate. Our results show that the transfer matrix method could serve as a versatile tool to study optical properties in graphene layers.

Acknowledgments

References

[1] Novoselov K S, Geim A K, Morozov S V, Jiang D, Zhang Y, Dubonos S V, Grigorieva I V and Firsov A A 2004 *Science* **306** 666
[2] Wilson M 2006 *Phys. Today* **59** 21
[3] Castro Neto A H, Guinea F, Peres N M R, Novoselov K S and Geim A K 2009 *Rev. Mod. Phys.* **81** 109
[4] Nair R R, Blake P, Grigorenko A N, Novoselov K S, Booth T J, Stauber T, Peres N M R and Geim A K 2008 *Science* **320** 1308
[5] Kuzmenko A B, van Heumen E, Carbone F and van der Marel D 2008 *Phys. Rev. Lett.* **100** 117401
[6] Stauber T, Peres N M R and Geim A K 2008 *Phys. Rev. B* **78** 085432
[7] Mak K F, Sfeir M Y, Wu Y, Lui C H, Misewich J A and Heinz T F 2008 *Phys. Rev. Lett.* **101** 196405
[8] Wang F, Zhang Y, Tian C, Girit C, Zettl A, Crommie M and Shen Y R 2008 *Science* **320** 206
[9] Li Z Q, Henriksen E A, Jiang Z, Hao Z, Martin M C, Kim P, Stormer H L and Basov D N 2008 *Nature Phys.* **4** 532
[10] Casiraghi C, Hartschuh A, Lidorikis E, Qian H, Harutyunyan H, Gokus T, Novoselov K S and Ferrari A C 2007 *Nano Lett.* **7** 2711
[11] Bae S *et al* 2010 *Nature Nanotechnol.* **5** 574
[12] Jo G *et al* 2010 *Nanotechnology* **21** 175201
[13] Xia F, Mueller T, Lin Y, Valdes-Garcia A and Avouris P 2009 *Nature Nanotechnol.* **4** 839
[14] Stauber T and Gómez-Santos G 2012 *Phys. Rev. B* **85** 075410
[15] Sun Z, Hasan T, Torrisi F, Popa D, Privitera G, Wang F, Bonaccorso F, Basko D M and Ferrari A C 2010 *ACS Nano* **4** 803
[16] Liu M, Yin X, Ulin-Avila E, Geng B, Zentgraf T, Ju L, Wang F and Zhang X 2011 *Nature* **474** 64
[17] Crassee I, Levallois J, Walter A L, Ostler M, Bostwick A, Rotenberg E, Seyller T, van der Marel D and Kuzmenko A B 2011 *Nature Phys.* **7** 48
[18] Ferreira A, Viana-Gomes J, Bludov Yu V, Pereira V, Peres N M R and Castro Neto A H 2011 *Phys. Rev. B* **84** 235410
[19] Wunsch B, Stauber T, Sols F and Guinea F 2006 *New J. Phys.* **8** 318
[20] Hwang E H and Das Sarma S 2007 *Phys. Rev. B* **75** 205418
[21] Mikhailov S A and Ziegler K 2007 *Phys. Rev. Lett.* **99** 016803
[22] Liu Y, Willis R F, Emtsev K V and Seyller T 2008 *Phys. Rev. B* **78** 201403
[23] Jablan M, Buljan H and Soljačić M 2009 *Phys. Rev. B* **80** 245435
[24] Profumo R E V, Polini M, Asgari R, Fazio R and MacDonald A H 2010 *Phys. Rev. B* **82** 085443
[25] Fei Z *et al* 2011 *Nano Lett.* **11** 4701
[26] Raether H 1998 *Surface Plasmons* (Berlin: Springer)
[27] Barnes W L, Dereux A and Ebbesen T W 2003 *Nature* **424** 824
[28] Maier S A 2007 *Plasmonics: Fundamentals and Applications* (New York: Springer)
[29] Ju L *et al* 2011 *Nature Nanotechnol.* **6** 630
[30] Vakil A and and Engheta N 2011 *Science* **332** 1291
[31] Nikitin A Y, Guinea F, García-Vidal F J and Martín-Moreno L 2011 *Phys. Rev. B* **84** 161407
[32] Thongrattanasiri S, Koppens F H L and García de Abajo F J 2012 *Phys. Rev. Lett.* **108** 047401
[33] Yan H, Li X, Chandra B, Tulevski G, Wu Y, Freitag M, Zhu W, Avouris P and Xia F 2012 *Nature Nanotechnol.* **7** 330
[34] Bonaccorso F, Sun Z, Hasan T and Ferrari A C 2010 *Nature Photon.* **4** 611
[35] Yeh P 1988 *Optical Waves in Layered Media* (New York: Wiley)

[36] Zi J, Wan J and Zhang C 1998 *Appl. Phys. Lett.* **73** 2084
[37] Jackson J D 2001 *Classical Electrodynamics* 3rd edn
     (New York: Wiley) p 16
[38] Saxon D S 1955 *Phys. Rev.* **100** 1771
[39] Ando T, Zheng Y and Suzuura H 2002 *J. Phys. Soc. Japan*
     71 1318
[40] Gusynin V P, Sharapov S G and Carbotte J P 2006 *Phys. Rev.
     Lett.* **96** 256802
[41] Falkovsky L A and Varlamov A A 2007 *Eur. Phys. J.* B **56** 281
[42] Ludwig A and Webb K J 2011 *Opt. Lett.* **36** 106
[43] Stern F 1967 *Phys. Rev. Lett.* **18** 546
[44] Das Sarma S and Hwang E H 2009 *Phys. Rev. Lett.*
     106 206412
[45] Yablonovitch E 1987 *Phys. Rev. Lett.* **58** 2059

[46] John S 1987 *Phys. Rev. Lett.* **58** 2486
[47] Joannopoulos J D, Johnson S G, Winn J N and Meade R D
     2008 *Photonic Crystals: Molding the Flow of Light* 2nd edn
     (Princeton, NJ: Princeton University Press)
[48] Falkovsky L A and Pershoguba S S 2007 *Phys. Rev.* B
     76 153410
[49] Kaipa C S R, Yakovlev A B, Hanson G W, Padooru Y R,
     Medina F and Mesa F 2012 *Phys. Rev.* B **85** 245407
[50] Pendry J B, Holden A J, Stewart W J and Youngs I 1996 *Phys.
     Rev. Lett.* **76** 4773
[51] Xu X, Xi Y, Han D, Liu X, Zi J and Zhu Z 2005 *Appl. Phys.
     Lett.* **86** 091112
[52] Zhan T R, Zhao F Y, Hu X H, Liu X H and Zi J 2012 *Phys.
     Rev.* B **86** 165416